Int. J. Electrochem. Sci., 17 **(2022)** Article Number: 220431, doi: 10.20964/2022.04.53

International Journal of
ELECTROCHEMICAL
SCIENCE
www.electrochemsci.org

A Novel BCRLS-BP-EKF Method for the State of Charge Estimation of Lithium-ion Batteries

Chao Wang, Shunli Wang[*], *Jinzhi Zhou, Jialu Qiao*

School of Information Engineering, Southwest University of Science and Technology, Mianyang 621010, China
[*]E-mail: 497420789@qq.com

Received: 6 December 2021 / *Accepted:* 18 January 2022 / *Published:* 4 March 2022

State-of-charge of lithium-ion batteries is one significant state parameter for battery management system monitoring. To accurately estimate the state-of-charge in real time, a novel BCRLS-BP-EKF method is proposed innovatively. Based on FFRLS algorithm, bias compensation is added to better capture the real-time operating characteristics of the system. To modify the model error of EKF algorithm, BP neural network is introduced, which has powerful nonlinear mapping and self-learning ability. The estimation error of EKF can be corrected by its learning and training relevant parameters that affect the estimation value of filtering. The data of different complex working conditions are used to verify the feasibility and rationality of the proposed algorithm by building a second-order RC equivalent circuit model. The results show that the root mean square error of the novel BCRLS-BP-EKF method under HPPC and BBDST operating condition can be controlled within 0.11% and 1.41% in state-of-charge estimation, which verifies that the proposed algorithm in this research has high precision and convergence characteristics. The novel BCRLS-BP-EKF method lays a theoretical foundation for accurate state estimation of lithium-ion batteries, which will effectively improve the security and reliability of electric vehicles.

Keywords: lithium-ion battery; second-order RC model; BCRLS; BP-EKF; state of charge

1. INTRODUCTION

With the emergence of global warming and various extreme weather, the problem of climate change and the shortage of energy supply has once again attracted widespread attention in society. Electric vehicles have the advantages of low noise, low pollution, low cost, easy maintenance and other advantages, which have gradually become a necessary vehicle for people's daily travel [1-3]. The lithium-ion battery has been widely applied in electric vehicles on account of long cycle life, high energy density, high rated voltage and low self-discharge rate [4, 5]. State of Charge (SOC) is one of the important indicators to measure the state of the battery. Accurate and real-time estimation of SOC is an

important premise to ensure the safety and health of the battery, as well as the necessary basis to ensure the safety of electric vehicles [6-8].

The commonly used SOC estimation algorithms include traditional estimation method, model-based method and data-driven method [9, 10]. Traditional estimation methods include ampere-hour (Ah) integration, open-circuit voltage (OCV) method and internal resistance method [11-13]. Model-based estimation methods are widely used at present, which are usually combined with equivalent circuit models and various filtering algorithms to estimate state variables [14]. Among them, Kalman filter algorithm is the most widely used, its core idea is to make the optimal estimation of the state of the system in the sense of minimum variance [15]. To better adapt to the nonlinear system of battery, the extended Kalman filter (EKF) algorithm and the unscented Kalman filter (UKF) algorithm are proposed [16-18]. However, considering the defects of various Kalman algorithms, there is still much room for improvement. The data-driven method is a hot topic and trend of current research [19, 20]. Due to the complex internal structure of lithium battery, it has strong nonlinear behavior. However, this method ignores the chemical and physical reactions inside the battery, thus avoiding battery modeling, but its physical significance is not obvious and it lacks effective theoretical support. The back propagation (BP) neural network has a strong nonlinear mapping ability and is especially suitable for dealing with the nonlinear internal structure of lithium batteries [21]. Chen et al. use BP neural network to estimate SOC, which improves the estimation accuracy of SOC to a certain extent [22]. However, BP neural network has a slow convergence speed, and the output results are random, and the error may be large.

To better characterize the battery characteristics, in this research, the second-order RC equivalent circuit model is constructed, the bias compensation recursive least square (BCRLS) algorithm is introduced innovatively to identify the parameters online precisely. To estimate the battery state-of-charge accurately, the BP-EKF method is proposed, which aims at the shortcomings of the EKF to deal with the nonlinear system and the defects of BP neural network. Considering that EKF has fast convergence speed and stable output results, and BP neural network has strong nonlinear processing ability, the two can be combined to make up for their shortcomings.

2. MATHEMATICAL ANALYSIS

2.1 Second-order RC equivalent modeling

The equivalent circuit model simulates the physical and chemical reactions inside the battery through components such as resistors and capacitors to characterize the nonlinear working principle of the battery [23]. The commonly used equivalent circuit models include Thevenin model, second-order RC model and PNGV model [24]. The more complex the model, the more accurate the nonlinear characteristics of the battery, but the corresponding calculation and parameter identification are also larger. Considering the difficulty of calculation and identification comprehensively, the second-order RC equivalent circuit model is selected in this paper, which has high simulation accuracy and moderate difficulty of calculation, and is suitable for the application of practical scenes. The second-order RC equivalent circuit model is shown in Figure 1.

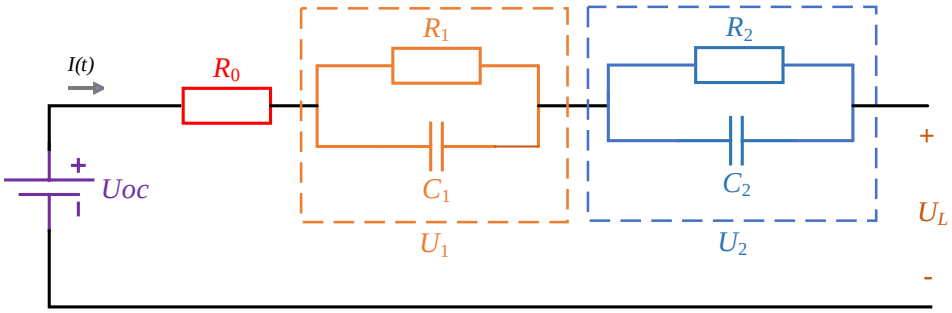

Figure 1. Second-order RC equivalent circuit model

In Figure 1, the open-circuit voltage (OCV) is represented by U_{OC}, the terminal voltage is represented by U_L, the ohmic internal resistance is represented by R_0, where R_1 and R_2 represent the polarization resistance, C_1 and C_2 represent the polarization capacitance. R_1C_1 loop represents the stage of rapid voltage change in the process of chemical reaction inside the battery, and R_2C_2 loop represents the stage of slow voltage change in the process of chemical reaction inside the battery. Let the current I is in the positive direction when discharging, the voltage and current expression of the second-order RC equivalent model can be obtained from Kirchhoff circuit law, as shown in Equation 1.

$$\begin{cases} U_L = U_{OC} - IR_0 - U_1 - U_2 \\ \dfrac{dU_1}{dt} = \dfrac{I}{C_1} - \dfrac{U_1}{R_1C_1} \\ \dfrac{dU_2}{dt} = \dfrac{I}{C_2} - \dfrac{U_2}{R_2C_2} \end{cases} \quad (1)$$

In Equation 1, U_1 and U_2 are the terminal voltages of the two RC loops respectively, and the open-circuit voltage U_{OC} can be represented by SOC in the state of charge. $[SOC, U_1, U_2]^T$ is selected as the state variable, and the equivalent circuit is discretized. The discretized state space expression is shown in Equation 2.

$$\begin{cases} \begin{bmatrix} SOC_{k+1} \\ U_{1,k+1} \\ U_{2,k+1} \end{bmatrix} = \begin{bmatrix} 1 & 0 & 0 \\ 0 & e^{-\frac{\Delta t}{\tau_1}} & 0 \\ 0 & 0 & e^{-\frac{\Delta t}{\tau_2}} \end{bmatrix} \begin{bmatrix} SOC_k \\ U_{1,k} \\ U_{2,k} \end{bmatrix} + \begin{bmatrix} -\dfrac{\eta \Delta t}{Q_N} \\ R_1\left(1 - e^{-\frac{\Delta t}{\tau_1}}\right) \\ R_2\left(1 - e^{-\frac{\Delta t}{\tau_2}}\right) \end{bmatrix} I_k + w_k \\ U_{L,k+1} = \begin{bmatrix} \dfrac{\partial U_{OC}}{\partial SOC} & -1 & -1 \end{bmatrix} \begin{bmatrix} SOC_k \\ U_{1,k} \\ U_{2,k} \end{bmatrix} - IR_0 + v_k \end{cases} \quad (2)$$

In Equation 2, Δt represents the sampling interval, τ is the time constant, $\tau_1 = R_1C_1$, $\tau_2 = R_2C_2$. W_k and V_k are state error and measurement error respectively. The rated battery capacity is represented by Q_N, and η is coulomb efficiency.

2.2 Parameter identification based on BCRLS

Recursive least square (RLS) algorithm is developed based on adaptive filtering theory [25]. Its basic principle is to estimate the coefficient on the premise of known input and output, to minimize the sum of squares of the difference between the actual value and the estimated value. This method is widely used in the field of system identification by modifying and updating the system parameters continuously to obtain the real-time characteristics of the system accurately. Due to filter saturation phenomenon in RLS algorithm, which will weaken the ability of data correction and eventually lead to larger parameter identification error [26]. Forgetting factor recursive least square (FFRLS) is introduced to reduce the influence of old data and enhance the feedback effect of new data, thus improving the online estimation ability of RLS. However, in the actual scene, the environment of lithium batteries is complex and changeable, and there will always be a lot of uncertain noise influence in the process of use, so the results identified by FFRLS are no longer unbiased [27]. Therefore, this paper introduces the bias compensation recursive least square (BCRLS) algorithm, which adds the bias compensation based on FFRLS to better capture the real-time operation characteristics of the system. The recursive process of BCRLS is shown in Figure 2.

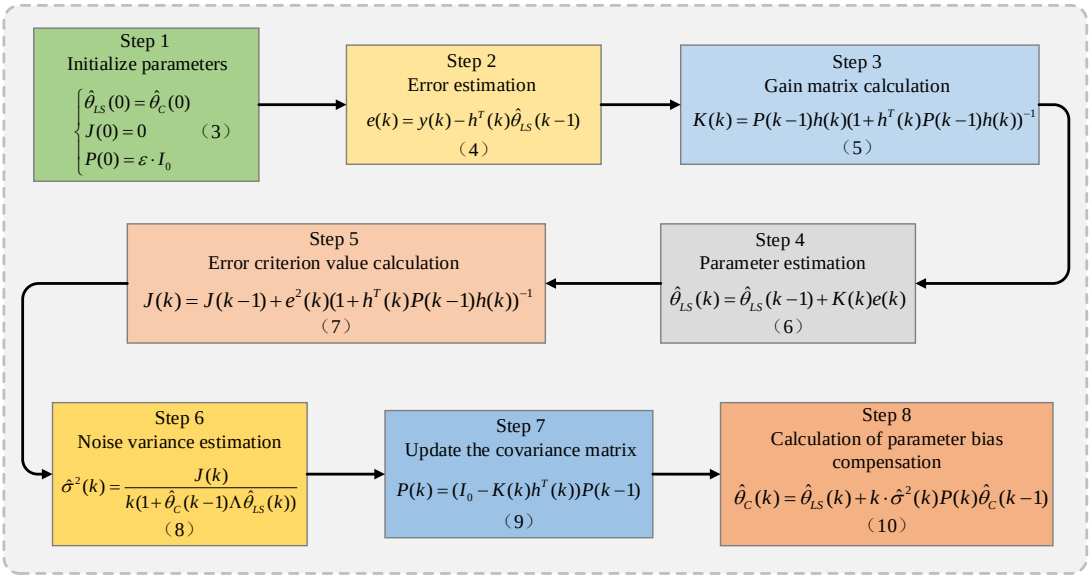

Figure 2. The process of BCRLS Recursive calculation

It can be seen from Figure 2 that the iterative calculation of BCRLS algorithm is divided into 8 steps, and every 8 steps is a cyclic iteration. Where, in Equation 3~10, $\hat{\theta}_{LS}$ represents the estimated parameter of FFRLS, $\hat{\theta}_C$ represents estimated parameters after bias compensation, K is the gain matrix, P is the covariance matrix, J is the output error criterion function, I_0 is the identity matrix, e is innovation matrix, $\hat{\sigma}^2$ is noise variance, Λ is the correlation matrix, and ε is a positive number, larger when the initial parameter is unknown and smaller when the initial parameter is known.

2.3 BP-EKF joint SOC estimation strategy

BP neural network is a kind of multi-layer feedforward neural network, which is mainly characterized by signal forward transmission and error back propagation [28]. It is composed of input layer, hidden layer and output layer [29]. Generally, parameters with high correlation with output expected value are selected as the input of neural network, and the correlation between output values should be as small as possible. The main function of the hidden layer is to deal with nonlinear problems, which can be set according to the complexity of the problem. BP neural network training, the first step is the forward propagation process, input data signal from the input layer into the neural network, layer by layer through the hidden layer until the output layer. The weights and thresholds of the network are adjusted according to the prediction errors so that the predicted output of BP neural network is approaching the desired output. Because the interior of lithium battery is a nonlinear system, it is especially suitable for BP neural network processing. The model structure of BP neural network for SOC prediction is shown in Figure 3.

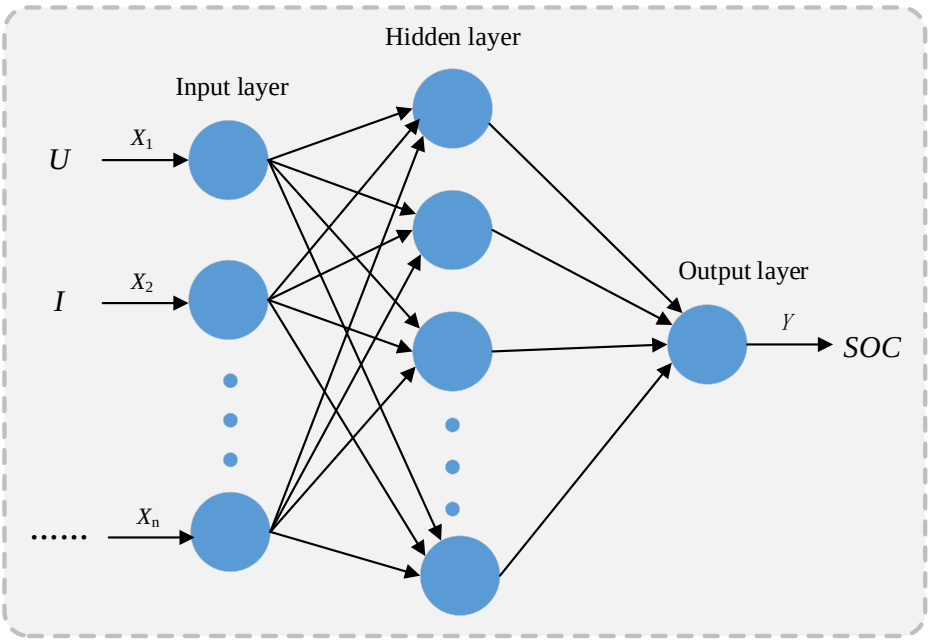

Figure 3. The model of BP neural network for SOC prediction

It can be seen from Figure 3 that the logical relationship among input layer, hidden layer and output layer of BP neural network. The input layer parameters are voltage, current, temperature, internal resistance and other parameters related to SOC estimation accuracy. The number of nodes in the hidden layer can be set according to the complexity of the processing problem and the number of input parameters. The output of the output layer is the prediction target SOC of the neural network.

Kalman filter (KF) is a filtering theory established by state space theory in time domain, which is mainly used to estimate linear time-invariant systems. The core algorithm is to obtain the state estimate corresponding to the minimum mean square error in finite iteration operation according to the principle of least mean square error, so that the estimated value is constantly close to the real state value [30].

When dealing with the nonlinear problem of lithium battery, the extended Kalman filter method adopts the first-order Taylor series expansion to linearize the nonlinear state space model, and then adopts the basic Kalman filter algorithm to implement it. Its iterative calculation process is shown in Figure 4.

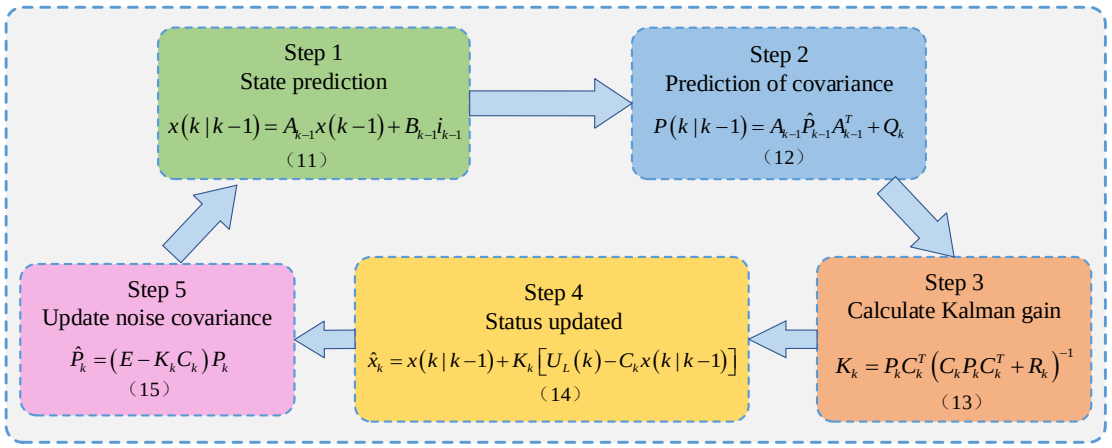

Figure 4. The process of Iterative calculation for EKF algorithm

It can be seen from Figure 4 that the iterative calculation of EKF algorithm is divided into 5 steps, and every 5 steps is a cyclic iteration. Where, in Equation 11~15, *x(k)* represents the state variable, A_k is the state transition matrix, B_k is the system control input matrix, i_k is the input current value, C_k is the system observation matrix, K_k is Kalman gain, P_k is error covariance matrix, Q_k is the expectation for noise of the system process, R_k is the expectation for noise of the system observation, $U_L(k)$ represents the real-time terminal voltage value, E is the identity matrix.

EKF algorithm has fast convergence speed and stable estimation results, but it ignores the higher-order terms of Taylor expansion when dealing with nonlinear systems, so there are certain model errors, which will indirectly lead to the decrease of the accuracy of the estimation results. In order to compensate the error of EKF model, BP neural network is introduced. With the powerful self-learning ability and nonlinear processing ability of neural network, the estimation error of EKF can be corrected by learning and training relevant parameters that affect the estimation value of filtering. The process of BP-EKF joint algorithm is shown in Figure 5.

There are three modules in Figure 5, BCRLS parameter identification module, EKF algorithm estimation module and BP-EKF error modification module, which collectively construct the BP-EKF joint algorithm.

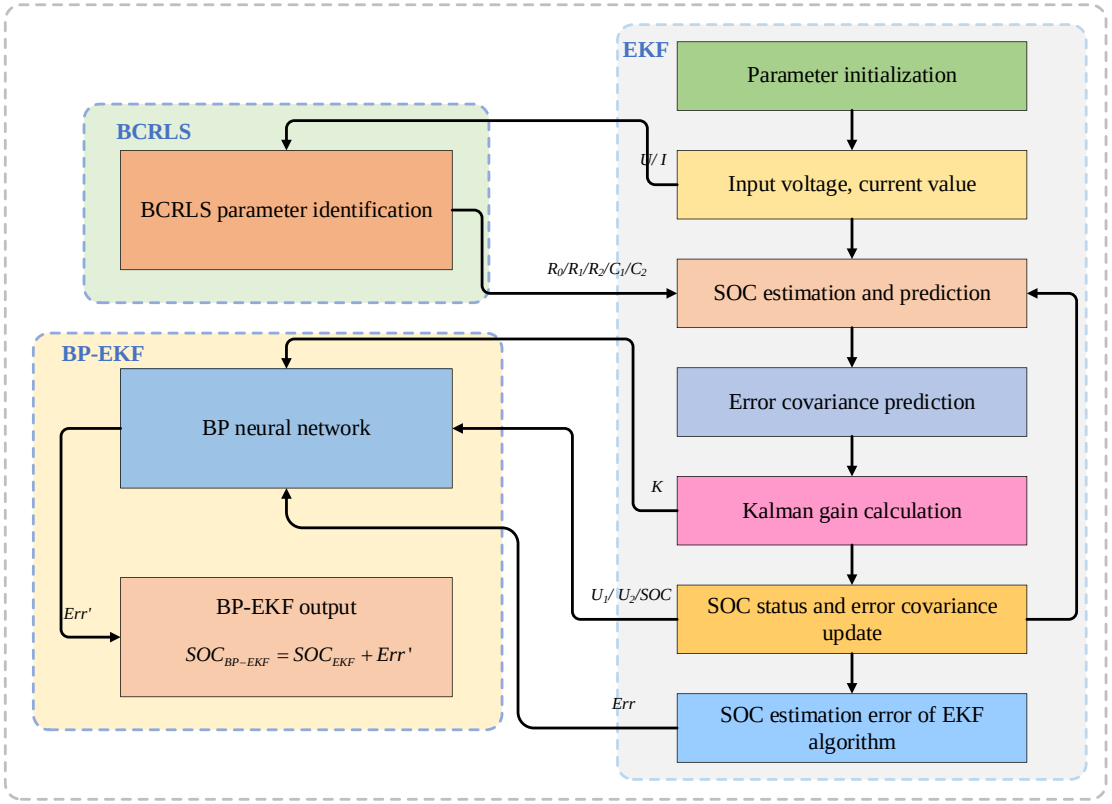

Figure 5. The process of BP-EKF joint algorithm

3. EXPERIMENTAL VERIFICATION

3.1 Experimental platform construction

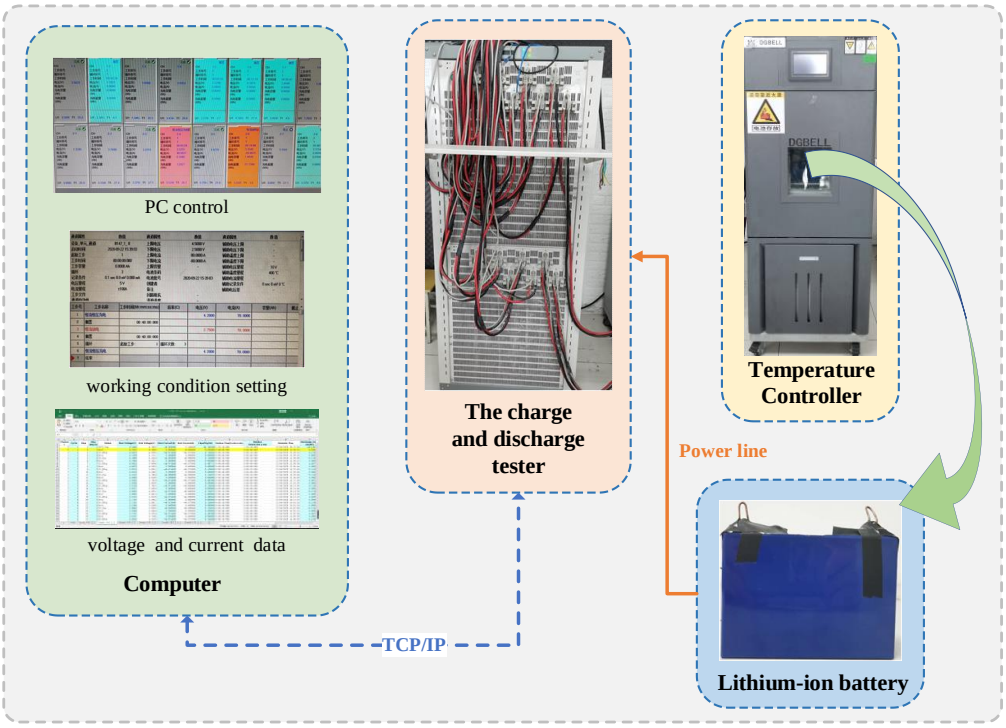

Figure 6. Experimental test platform

In this study, a ternary lithium-ion battery with a rated capacity of 50 Ah is taken as the experimental object, the voltage, current, capacity and other relevant data of charge and discharge under different working conditions is recorded through experiments. To obtain experimental data, an experimental platform is built with the BTS200-100-104 battery test device and temperature control equipment. The platform is shown in Figure 6.

As shown in Figure 6, working condition setting, charging and discharging test instrument and test data acquisition are controlled by computer terminal. The thermostat ensures constant temperature during battery testing.

3.2 Parameter identification experiment and analysis

The hybrid pulse power characterization (HPPC) working condition data at room temperature (25°C) are selected for online parameter identification of the model. The HPPC experiment steps are as follows:

Step 1. Charge the battery at constant current and constant voltage (4.2 V/1 C) until it is fully charged.

Step 2. After the battery is left for 40 min, the voltage at both ends of the battery is measured and recorded.

Step 3. Conduct current pulse experiment on the battery. First, charge the battery at a constant current of 1 C for 10 s, then stand for 40 s, and then charge the battery at a constant current of 1 C for 10 s to restore the power before discharge.

Step 4. Reduce the power of the battery by 10% at a constant discharge of 1 C for 6 min, and then stand for 40 min. The recording terminal voltage is the open-circuit voltage at this time.

Step 5. Repeat Step 3 and Step 4 10 times until the battery level is 0.

After the HPPC experimental data were collected, FFRLS algorithm and BCRLS algorithm were used to identify the parameters of the second-order model, to obtain the corresponding values of internal resistance R_0, polarization resistance R_1 and R_2, and polarization capacitance C_1 and C_2 of lithium battery at different times. Using these data as the input of the model, the real-time terminal voltage simulation value can be obtained through calculation, and the terminal voltage simulation value and the measured value are compared and analyzed to verify the effectiveness of the improved algorithm. The experimental results are shown in Figure 7.

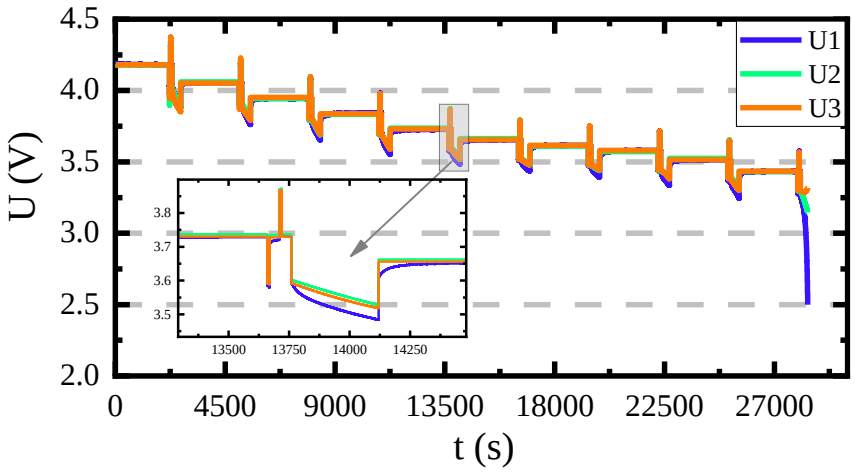

(A) Comparison of identification results of HPPC working condition

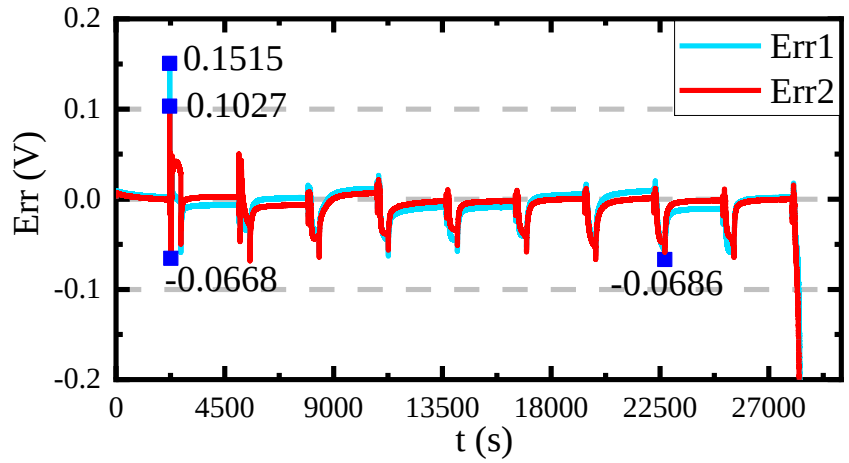

(B) Comparison of identification errors of HPPC working condition

Figure 7. Parameter identification result of HPPC working condition

Table 1. Comparison of identification errors analysis under HPPC working condition

Identification method	FFRLS	BCRLS
Mean Err	-0.77%	-0.75%
MAE	1.21%	1.19%
RMSE	2.63%	2.61%

Figure 7A shows the voltage comparison of parameter identification results of the two algorithms, where U1 represents the measured voltage, U2 represents the simulation voltage value identified by FFRLS, and U3 represents the simulation voltage value identified by BCRLS. In Figure 7B, Err1~Err2 represent the simulation voltage error curve corresponding to U2 ~U3. It can be seen that the initial voltage error of each charge and discharge cycle is relatively large, and the error at the end of the final discharge is also larger, which is caused by the violent chemical reaction inside the lithium-ion battery. While the error in the remaining part is smaller, and the simulation effect is better. Furthermore,

it can be seen from Table 1 that the mean error, mean absolute error and root mean square error of BCRLS are 0.02 percentage points smaller than FFRLS. The experimental results show that BCRLS algorithm has better parameter identification effect and higher precision.

3.3 Verification and analysis of BP algorithm

To better verify the superiority of BP-EKF algorithm, first of all, the BP neural network algorithm and EKF algorithm are analyzed experimentally. To verify the effect of BP neural network, voltage and current are directly used as input of neural network, and SOC is used as output of neural network. The data under BBDST working conditions are taken as the training data of BP neural network, 85% are randomly selected as the training set and 15% as the verification set.

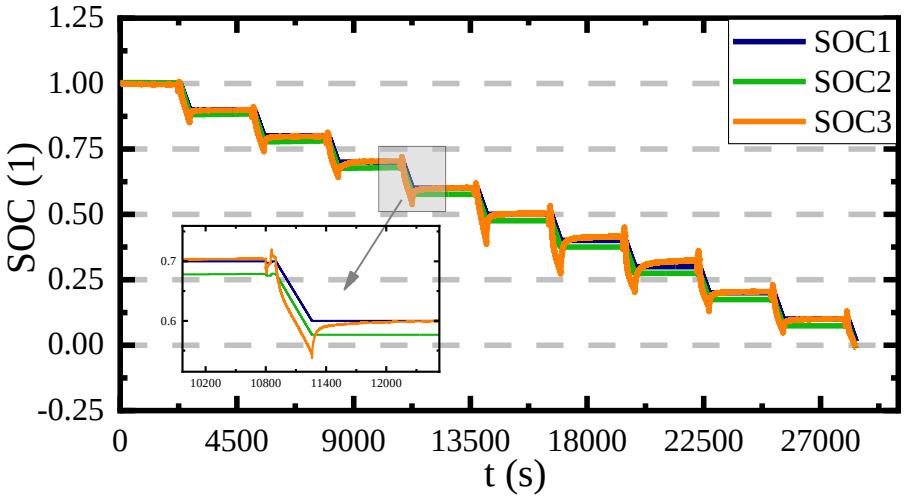

(A) Comparison of SOC estimation results with BP and EKF

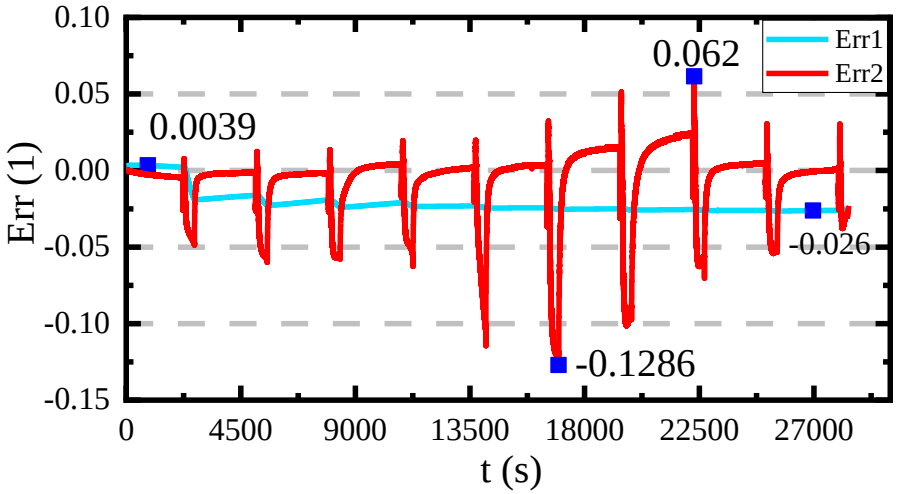

(B) Comparison of SOC estimation error with BP and EKF

Figure 8. SOC estimation results and errors of BP and EKF under HPPC working condition

The training times of BP neural network was set as 1000, the number of hidden layer nodes was set as 8, the learning rate was set as 0.01, and the training target error was set as 1e-7. After the neural

network training is completed, the data under HPPC condition is used to test， and the result is compared with the estimated value of EKF algorithm. The experimental results are shown in Figure 8 and Table 2.

Table 2. Comparison of experimental error analysis of BP and EKF under HPPC working condition

Estimation method	BP	EKF
Maximum Err	12.88%	4.08%
MAE	1.28%	1.94%
RMSE	2.47%	2.06%

As shown in Figure 8A, SOC1 represents the reference SOC value, SOC2 represents the SOC value of the EKF algorithm, and SOC3 represents the SOC estimated value of the BP neural network algorithm. In Figure 8B, Err1 and Err2 represent the estimation errors corresponding to SOC2 and SOC3 respectively. As can be seen from Figure 8A, BP neural network has poor SOC curve fitting effect in the pulse discharge stage, and the error is significantly greater than that of EKF algorithm. However, in the static stage after discharge, the SOC curve fitting effect is better, which is significantly better than that of EKF algorithm. According to the analysis in In Figure 8B and Table2, the error curve of EKF algorithm has small fluctuation and fast convergence and finally tends to be stable with a small error value. The error curve of BP neural network algorithm oscillates obviously, the convergence effect is poor and the error value is larger. In conclusion, BP neural network and EKF can be combined to improve the estimation accuracy of SOC.

3.4 Verification and analysis of BP-EKF algorithm

To verify the effectiveness and feasibility of BP-EKF algorithm, the data under Dynamic Stress Test (DST) operating condition is used as the training data of BP neural network. After screening, a total of 91343 groups of effective test data were selected under DST operating condition, 85% are randomly selected as the training set, 15% as verification set, the training times of BP neural network is set to 1000, the number of hidden layer nodes is set to 8, the learning rate is set to 0.001, and the training target error is set to 1e-7. Firstly, the initial estimate value is obtained by using EKF algorithm. Next, the Kalman gain K, the estimated value of SOC, the terminal voltage U1 and U2 of two RC loops are taken as input of BP neural network. The estimated error of SOC, namely Err, is taken as output of neural network. Then, BP neural network is trained according to the set parameters. For details, please refer to Figure 5.

3.4.1 HPPC working condition verification test

The trained neural network is verified with the data under HPPC working condition. There are 283665 groups of valid data, the verification results are shown in Figure 9 and Table 3.

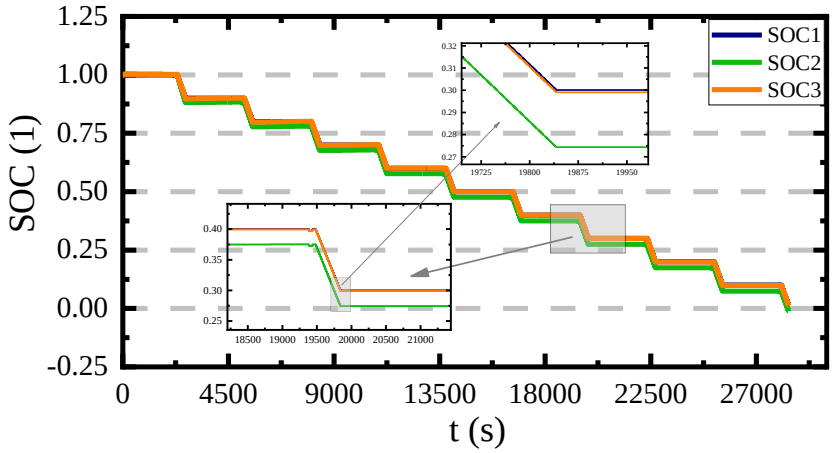

(A) Comparison of SOC estimation results with different algorithms

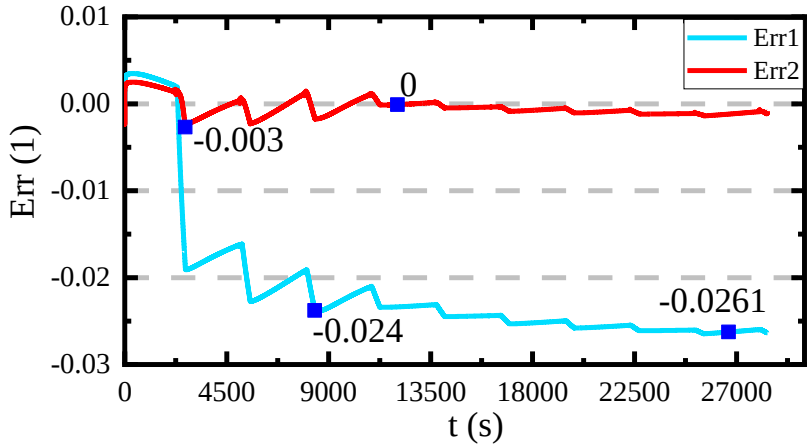

(B) Comparison of SOC estimation error with different algorithms

Figure 9. SOC estimation results and errors of HPPC working condition

Table 3. Comparison of experimental error analysis of different algorithms under HPPC working condition

Estimation method	EKF	BP-EKF
Maximum Err	2.65%	2.52%
MAE	2.17%	0.09%
RMSE	2.27%	0.11%

As shown in Figure 9A, SOC1 represents the reference SOC value, SOC2 represents the SOC value of the EKF algorithm, and SOC3 represents the SOC estimated value of the BP-EKF algorithm.

In Figure 9B, Err1 and Err2 represent the estimation errors corresponding to SOC2 and SOC3 respectively. It can be seen from Figure 9A that the curve fitting effect of BP-EKF algorithm is significantly better than that of EKF algorithm, and it almost coincides with the reference value curve, which fully reflects the significant error compensation effect of BP neural network. It can be seen from Figure 9B that the corresponding error curves of the two algorithms fluctuate in the early stage of discharge, but the fluctuation range of BP-EKF algorithm is significantly smaller. The error curves gradually tend to be stable at the middle and late discharge period, but the BP-EKF algorithm converges faster and the error is smaller. Furthermore, it can be analyzed from the Table 3 that the maximum error, the mean absolute error and root mean square error of BP-EKF algorithm under HPPC working condition are reduced by 0.13%, 2.08% and 2.16%, respectively, compared with EKF algorithm. The results show that BP-EKF has excellent tracking performance and stability performance.

3.4.2 BBDST working condition verification test

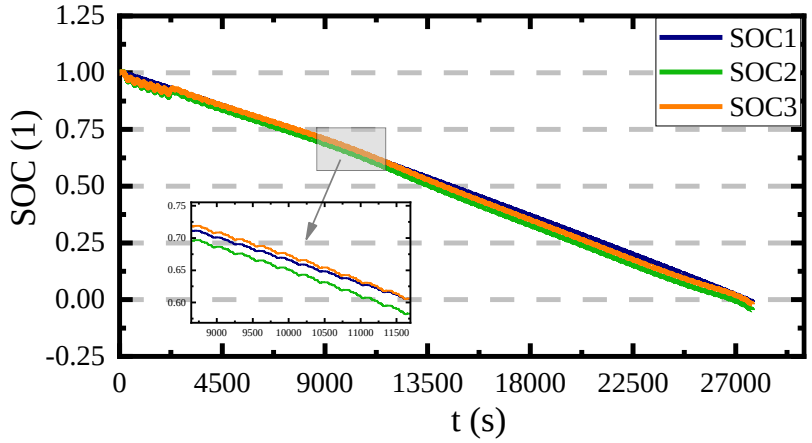

(A) Comparison of SOC estimation results with different algorithms

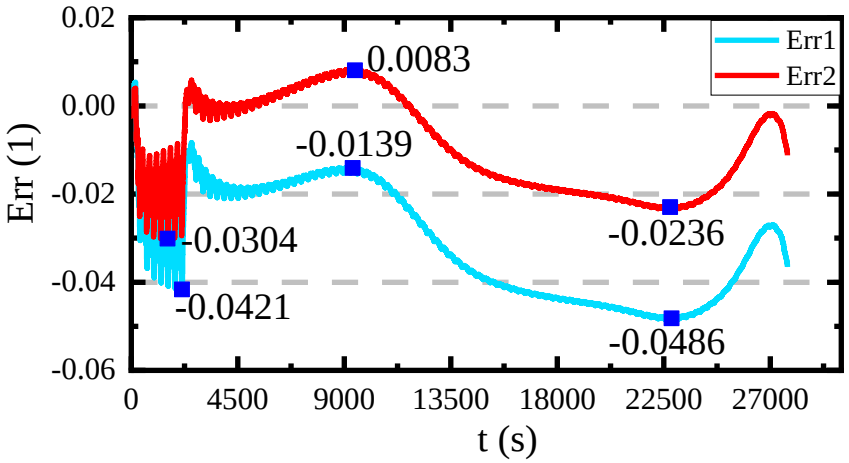

(B) Comparison of SOC estimation error with different algorithms

Figure 10. SOC estimation results and errors of BBDST working condition

The practical application condition of lithium-ion batteries is complex and changeable. BBDST working condition is obtained from the real data collection of the Beijing bus dynamic stress test,

including the data of the bus in the start, taxiing, acceleration, rapid acceleration, and other operations, which can verify the stability and strong tracking performance of the proposed algorithm. There are 277275 groups of valid data, the verification results are shown in Figure 10 and Table 4.

Table 4. Comparison of experimental error analysis of different algorithms under BBDST working condition

Estimation method	EKF	BP-EKF
Maximum Err	4.84%	3.01%
MAE	3.12%	1.16%
RMSE	3.36%	1.41%

As shown in Figure 10A, SOC1 represents the reference SOC value, SOC2 represents the SOC value of the EKF algorithm, and SOC3 represents the SOC estimated value of the BP-EKF algorithm. In Figure 10B, Err1 and Err2 represent the estimation errors corresponding to SOC2 and SOC3 respectively. It can be seen from Figure 10A that the SOC curve fitting degree of BP-EKF algorithm is closer to the reference truth value, reflecting its strong tracking ability. It can be seen from Figure 10B that the shapes and trends of the two sets of error curves are very similar, but the error value of BP-EKF algorithm is significantly smaller and closer to 0, reflecting the good self-learning ability and error correction ability of BP neural network. At the beginning and end of discharge, the error curves of the two algorithms fluctuate widely, which is caused by the violent chemical reaction inside the battery. Furthermore, it can be analyzed from the Table 3 that the maximum error, the mean absolute error and root mean square error of BP-EKF algorithm under BBDST operating condition are reduced by 1.83%, 1.96% and 1.95%, respectively, compared with EKF algorithm. The results show that BP-EKF has better tracking performance and stability performance.

4. CONCLUSIONS

The SOC estimation accuracy of lithium-ion batteries directly determines the quality of battery management system, and the accuracy of battery equivalent model and parameter identification will affect the SOC estimation accuracy. In this research, the second-order RC model is applied to characterize the state and characteristics of the battery, and the BCRLS method is applied for online parameter identification, which effectively improves the accuracy of online parameter identification. To improve the estimation accuracy of SOC, a novel joint algorithm for modifying and optimizing EKF based on BP neural network is proposed. The relevant parameters affecting the estimation of EKF algorithm are trained by BP neural network, and the error of EKF algorithm is compensated. The experimental data of HPPC and BBDST operating conditions are used for verification, the results show that the RMSE of the novel BCRLS-BP-EKF algorithm under HPPC and BBDST condition can be controlled within 0.11% and 1.41% in SOC estimation, the accuracy and performance are greatly

improved. The paper not only lays a foundation for further research on battery health state and optimization of battery management system but also has positive significance for the further development of new energy vehicles.

References

1. Y. Hua, S. Zhou, H. Cui, X. Liu, C. Zhang, X. Xu, H. Ling and S. Yang, *International Journal of Energy Research*, 44 (2020) 11059.
2. S. Pourjafar, H. Shayeghi, F. Sedaghati, S. Seyedshenava and F. Blaabjerg, *International Journal of Circuit Theory and Applications*, 49 (2021) 2453.
3. S. A. Hasib, S. Islam, R. K. Chakrabortty, M. J. Ryan, D. K. Saha, M. H. Ahamed, S. I. Moyeen, S. K. Das, M. F. Ali, M. R. Islam, Z. Tasneem and F. R. Badal, *Ieee Access*, 9 (2021) 86166.
4. M. Al-Gabalawy, N. S. Hosny, J. A. Dawson and A. I. Omar, *International Journal of Energy Research*, 45 (2021) 6708.
5. L. Chen, S. Wang, H. Jiang, C. Fernandez and X. Xiong, *International Journal of Electrochemical Science*, 16 (2021) 1.
6. W. Xu, S. Wang, C. Jiang, C. Fernandez, C. Yu, Y. Fan and W. Cao, *International Journal of Energy Research*, 45 (2021) 14592.
7. J. Qiao, S. Wang, C. Yu, W. Shi and C. Fernandez, *International Journal of Circuit Theory and Applications*, 49 (2021) 3879.
8. C. Jiang, S. Wang, B. Wu, C. Fernandez, X. Xiong and J. Coffie-Ken, *Energy*, 219 (2021) 1.
9. H. Wang, Y. Zheng and Y. Yu, *Processes*, 9 (2021) 1.
10. X. Xin, S.-L. Wang, C.-M. Yu, J. Cong and J. Coffie-Ken, *International Journal of Electrochemical Science*, 15 (2020) 2226.
11. Z. Ren, C. Du, Z. Wu, J. Shao and W. Deng, *International Journal of Energy Research*, 45 (2021) 13692.
12. Y. Wang, L. Zhao, J. Cheng, J. Zhou and S. Wang, *Applied Sciences-Basel*, 10 (2020) 1.
13. Y. Li, G. Xu, B. Xu and Y. Zhang, *International Journal of Electrochemical Science*, 16 (2021) 1.
14. Y. Wang, J. Tian, Z. Sun, L. Wang, R. Xu, M. Li and Z. Chen, *Renewable & Sustainable Energy Reviews*, 131 (2020) 1.
15. J. Duan, P. Wang, W. Ma, X. Qiu, X. Tian and S. Fang, *Energies*, 13 (2020) 1.
16. Z. He, Y. Li, Y. Sun, S. Zhao, C. Lin, C. Pan and L. Wang, *Journal of Energy Storage*, 39 (2021) 1.
17. Z. Chen, L. Yang, X. Zhao, Y. Wang and Z. He, *Applied Mathematical Modelling*, 70 (2019) 532.
18. N. Peng, S. Zhang, X. Guo and X. Zhang, *International Journal of Energy Research*, 45 (2021) 975.
19. Y. Qin, S. Adams and C. Yuen, *Ieee Transactions on Industrial Informatics*, 17 (2021) 7304.
20. M. Jiao, D. Wang, Y. Yang and F. Liu, *Engineering Applications of Artificial Intelligence*, 104 (2021) 1.
21. Y. Li, W. Wang, C. Lin and F. Zuo, *Science China-Technological Sciences*, 64 (2021) 2373.
22. X. Chen, S. Wang, Y. Xie, C. Fernandez and Y. Fan, *International Journal of Electrochemical Science*, 16 (2021) 1.
23. Y. Fang, Q. Zhang, H. Zhang, W. Xu, L. Wang, X. Shen, F. Yun, Y. Cui, L. Wang and X. Zhang, *Iet Power Electronics*, 14 (2021) 1515.
24. D. Liu, Y. Fan, S. Wang, L. Xia, J. Qiu and E. D. Bobobee, *International Journal of Electrochemical Science*, 16 (2021) 1.
25. M. Li, Y. Zhang, Z. Hu, Y. Zhang and J. Zhang, *Sensors*, 21 (2021) 1.
26. S.-C. Chan, J.-Q. Lin, X. Sun, H.-J. Tan and W.-C. Xu, *Ieee Transactions on Instrumentation and Measurement*, 69 (2020) 4555.
27. W. Xiong, Y. Mo and C. Yan, *Mathematical Problems in Engineering*, 2020 (2020) 1.

28. Y. Zhang, S. Wang, W. Xu, C. Fernandez and Y. Fan, *International Journal of Electrochemical Science*, 16 (2021) 1.
29. S. Zhang, X. Guo and X. Zhang, *Advances in Electrical and Computer Engineering*, 19 (2019) 3.
30. M. Wu, L. Qin, G. Wu, Y. Huang and C. Shi, *Journal of Energy Storage*, 41 (2021) 1.